The *Pyxis* Interferometer and Beam Combiner

Jonah Hansen

Australian National University

Thesis Proposal

Supervisor: A/Prof Michael Ireland
Associate Supervisor: Dr Tony Travouillon
Associate Supervisor: Dr Tiphaine Lagadec

Research School of Astronomy and Astrophysics
College of Science
The Australian National University
Canberra, Australia

4 July 2020

Abstract

This proposal outlines a PhD project primarily associated with *Pyxis*, a new interferometer planned to be built at Mt Stromlo Observatory. *Pyxis* is primarily designed to be a ground technological prototype for a formation flying space interferometer mission, testing a new metrology and control system while performing unique science through optical interferometric polarimetry. This project will focus in particular on building the scientific beam combiner for the instrument; a system that will combine light from the two arms of the interferometer and extract visibility and polarimetry information by analysing the resultant fringes. In the process, the project will investigate multiple options for a fringe tracking system, as well as a choice of beam combination scheme. Furthermore, the project will also include participating in testing *Pyxis* as a whole and conducting the first observing campaign. With *Pyxis* having the opportunity to fill the instrumentation niche of optical interferometric polarimetry, there is ample scope for scientific goals as well; in particular to analyse the scattered light structures around M giant and supergiant stars such as Mira variables and Betelgeuse. Furthermore, if the sensitivity of *Pyxis* is sufficient, there is also opportunity to examine the disks surrounding Herbig Ae/Be stars. Overall, this is an ambitious project that ties together novel instrumentation and interesting science on giant stars.

Contents

Section 1

Motivation

Pyxis is an upcoming robotic interferometer to be built at the Australian National University, and the main component of my PhD project. This interferometer is primarily designed to demonstrate a metrology system and formation flying approach for a future space interferometer mission, while also tackling interesting science cases revolving around resolving dust and scattered light structures around giant stars. This section details the motivation behind *Pyxis*, in particular why space interferometry is a required future technology and why a pathfinder such as *Pyxis* is needed. The text is adapted from Hansen (2019) and Hansen and Ireland (2020).

1.1 The Case for Space Interferometry

Since the first confirmed exoplanet detection of 51 Peg b by Mayor and Queloz (1995), there has been a desire to directly image and study exoplanets without relying on indirect methods such as transit (e.g. Borucki et al., 2010) and radial velocity (e.g. Mayor et al., 2003) measurements. While these methods have produced a large number of exoplanet detections since 51 Peg b, they are limited by selection biases and do not allow many of the properties of the planet to be studied. In particular, one of the major goals of exoplanet research is identifying potentially habitable worlds that may harbour life. To determine this, one would need to study the atmosphere of the planet. Transmission spectroscopy is especially promising for characterisation of hydrogen rich atmospheres, but is challenging for terrestrial atmospheres (e.g. Diamond-Lowe et al., 2019). This is where direct imaging becomes important - by directly imaging an exoplanet, it is possible to obtain direct information about the atmosphere and surface of terrestrial systems.

However, many obstacles stand in the way of the direct imaging of an exoplanet. One of the most prominent of these concerns separating the emission of the planet from that of its host star. The contrast between a star and a 300 K terrestrial planet (using the Sun/Earth ratio as an analogue) is an astounding 10^{10} in visible light, but viewing in the mid-infrared (10 μm) reduces the contrast to 10^{7} (Angel and Woolf, 1997). There are other reasons for choosing the mid-infrared as well - in particular the presence of strong molecular atmospheric lines such as CH_4 at 7.7 μm, O_3 at 9.7 μm, N_2O at 7.8 μm and CO_2 at 15 μm.

While the mid-infrared contains many advantages over the visible, there are still two main complications for imaging in this part of the spectrum. The first issue is the substantial thermal background that interferes with ground based telescopes, requiring space-based telescopes located far from the Earth to achieve zodiacal-limited observations. The second issue concerns the baselines required to achieve high angular resolution: for a planet 1 AU out from a host star at 10 pc, a minimum angular resolution of 0.1 " would be required to distinguish the planet from the star. For a coronagraphic inner working angle of 2 λ/D and a 15 μm wavelength, detecting such an exoplanet would require a 60 m telescope. With interferometry, one can achieve high spatial resolution with small apertures, circumnavigating the issues of a monolithic telescope with such a resolution requirement and especially for space-based monolithic telescopes (Angel and Woolf, 1997). A mid-infrared interferometer would be complementary to an optical/near-infrared coronagraph space telescope, and would detect more planets around cool stars in particular (Quanz et al., 2018). This is significant as the costs for a large scale space-based mid-infrared interferometric mission (such as *Darwin*) would be more economical ($\sim$\$1.2 B (Cockell et al., 2009)) than the equivalent space-based optical telescope (e.g. *LUVIOR* at $>$ \$10 B (National Aeronautics and Space Administration, 2019)).

To summarise, mid-infrared space interferometry is the inevitable endpoint of high angular resolution astrophysics, as it mitigates the issues surrounding angular resolution and sensitivity that currently plague modern ground and space-based telescopes. It is thus a key technology that can be leveraged to analyse exoplanet formation and atmospheres with exceptional detail in a relatively cost effective manner.

Space interferometry was studied in detail throughout the 1990s and early 2000s, in particular with NASA's Terrestrial Planet Finder (*TPF*) mission (Beichman et al., 1999), NASA's Space Interferometry Mission (*SIM*) (Shao, 1998) and ESA's *Darwin* mission (Léger et al., 1996), but due to budget costs and technology unreadiness, these concepts were dropped. However, the field is now at the start of a resurgence, with the *Darwin*-like mission *LIFE* (Large Interferometer For Exoplanets) (Quanz et al., 2018; Quanz et al., 2019) in discussion for ESA's Voyage 2050 plan. To approach technological readiness for such a mission, smaller pathfinder studies must be undertaken. One of the more critical of these is formation flying interferometry - keeping multiple satellites in formation at the required stability level to perform interferometry. Such a potential satellite mission (temporarily named *ASP*) is discussed in Hansen and Ireland (2020). After this point, another larger scale mission could be studied, namely a space-based version of the Planet Formation Imager (Monnier et al., 2018). This would act as being a final stepping stone between technology demonstration and the final *LIFE* mission. A summary of the cancelled and planned space interferometry missions can be found in Figure 1.1.

Even before launching a satellite though, it is critical to test whether the formation flying control system, including metrology (knowing the relative locations of the satellites) will be sufficiently

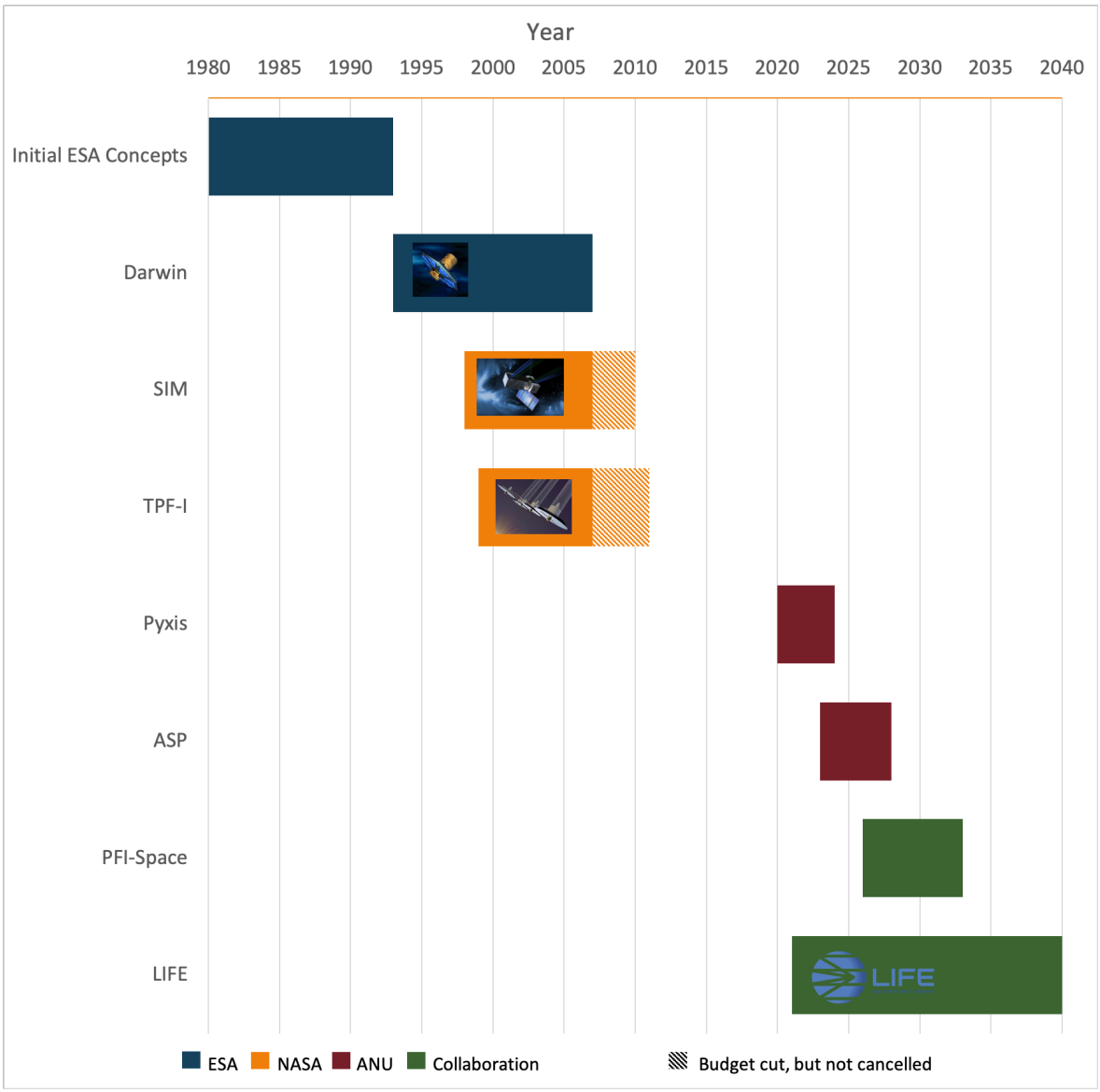

Figure 1.1: Timeline of past and proposed space interferometry missions.

stable for interferometry. This is the primary goal of the *Pyxis* interferometer - to demonstrate a formation flying architecture on the ground that can then be translated into a small CubeSat mission such as in Hansen and Ireland (2020). Such an interferometer will also be able to conduct some unique science, in particular high angular resolution spectropolarimetry of large stars. My PhD project will focus on designing this science instrument for *Pyxis*, and will be explored in Section 3.

Section 2

A Brief Look at Optical Stellar Interferometry

In this section, I will describe some of the relevant literature related to the instrumentation component of my project, covering both optical interferometry and beam combination.

Optical interferometry is the science of measuring the interference of waves in the visible and near infrared part of the electromagnetic spectrum, and is an important tool in stellar astrophysics. Since the first direct measurement of a star's diameter by Michelson and Pease (1921), optical stellar interferometry has paved the way to provide a relatively cost effective way to obtain high resolution measurements without requiring a telescope with an enormous primary mirror. Instead, two smaller apertures separated by a baseline B are used to obtain a resolution roughly equivalent of that of a single mirror of diameter B. The drawback to interferometry, however, is that while the resolution is equivalent to such a telescope, the sensitivity is greatly reduced due to only having the two smaller apertures of collecting area. Furthermore, the Earth's atmosphere causes more issues with an interferometer than the equivalent monolithic telescope as we will explore later.

2.1 The Mathematics of Interferometry

We will start with the basic mathematics behind an interferometer. This material is adjusted from Hansen (2019), which in turn is based on Boden (2000). Consider two small apertures at positions $\mathbf{x_1}$ and $\mathbf{x_2}$, with the baseline between them being $\mathbf{B} = \mathbf{x_2} - \mathbf{x_1}$. Then, suppose that they are looking at a point source with position $\mathbf{s}$. This setup is illustrated in Figure 2.1, obtained from Boden (2000). From the scalar field approximation, the monochromatic electromagnetic fields at the apertures are proportional to:

$$E_1 \propto e^{-i\mathbf{k}\hat{\mathbf{s}}\cdot\mathbf{B}} e^{-i\omega t} \tag{2.1}$$

$$E_2 \propto e^{-i\omega t} \tag{2.2}$$

where $\mathbf{k}$ and ω are the angular wavenumber vector and angular frequency of the field respectively.

Now, let's say that each field is propagated through the two arms of the interferometer by different optical path lengths d_1 and d_2 respectively, right before the light from the two telescopes are

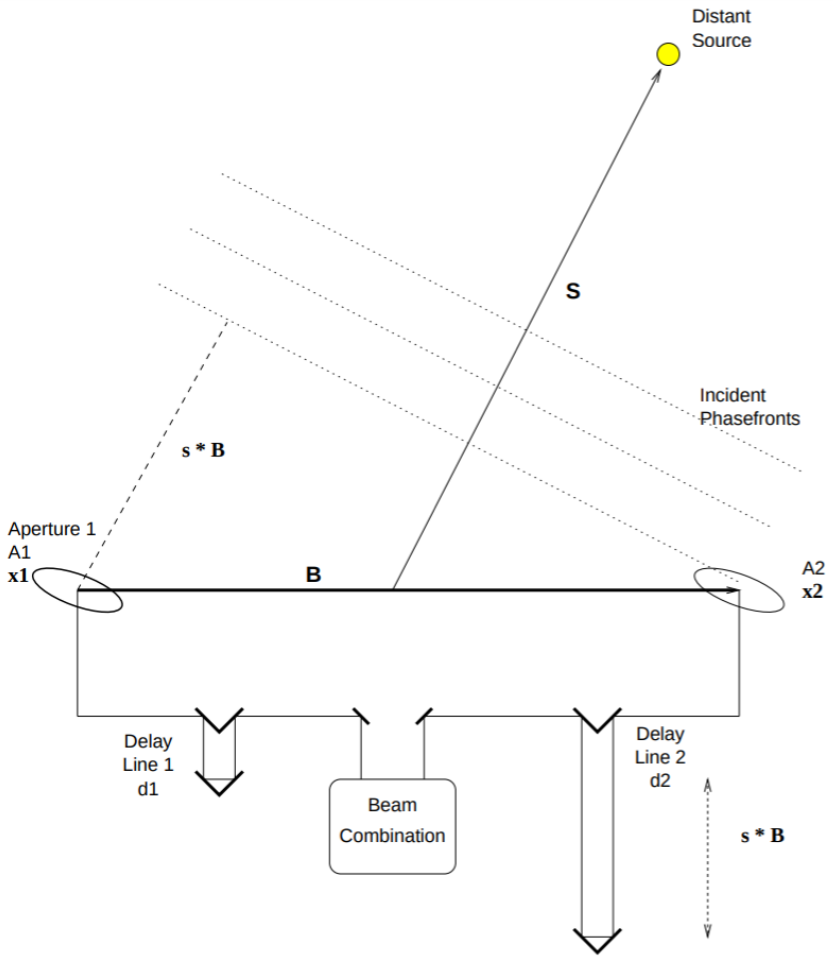

FIGURE 2.1: A simple interferometer setup, taken from Boden (2000). Here $\mathbf{B}$ represents the baseline of the interferometer, consisting of telescopes at $\mathbf{x_1}$ and $\mathbf{x_2}$. The position of the target star is denoted $\mathbf{s}$, and d_1/d_2 are the two different optical paths (modified through delay lines).

combined. The electric fields thus have an extra phase delay, and so can be described by:

$$E_1 \propto e^{-\mathbf{ik\hat{s}\cdot B}} e^{-i\omega t} e^{-ikd_1} \tag{2.3}$$

$$E_2 \propto e^{-i\omega t} e^{-ikd_2} \tag{2.4}$$

The interferometer detector measures the time averaged intensity of the superposition of the two incident electric fields (Haniff, 2007), and so the detected intensity is proportional to:

$$i = \langle |E_1 + E_2|^2 \rangle \tag{2.5}$$

$$\propto 2 + e^{-i(kd_1 + k\hat{\boldsymbol{s}}\cdot\boldsymbol{B} - kd_2)} + e^{i(kd_1 + k\hat{\boldsymbol{s}}\cdot\boldsymbol{B} - kd_2)} \tag{2.6}$$

$$\propto 1 + \cos\left(k(d_1 - d_2 + \hat{\mathbf{s}}\cdot\mathbf{B})\right) \tag{2.7}$$

The quantity $D = d_1 - d_2 + \hat{\mathbf{s}} \cdot \mathbf{B}$ is known as the optical path difference/delay of the measurement, and it can be seen that the intensity will vary harmonically with a period equal to the wavelength of light λ over the space of the delay. One period of this sinusoidal intensity pattern is known as a "fringe".

We now develop these concepts for an extended source. The brightness on the sky can be written as $I(\mathbf{s} = \mathbf{s_0} + \mathbf{\Delta s})$ where $\mathbf{s_0}$ is pointing towards the centre of the object and $\mathbf{\Delta s}$ perpendicular to this in the plane of the sky. We can assume that the extended source is just a number of point sources, and so we integrate the source intensity over the solid angle $d\Omega$ in the sky:

$$i(\mathbf{s_0}, \mathbf{B}) \propto \int I(\mathbf{s})[1 + cos(kD)]d\Omega \tag{2.8}$$

Haniff (2007) and Boden (2000) show that, assuming that the delays d_1 and d_2 are adjusted such that they cancel the geometric delay term $\mathbf{s_0} \cdot \mathbf{B}$ but still introduce a small path delay δ to one arm of the interferometer, the intensity can be written as:

$$i(\mathbf{s_0}, \mathbf{B}, \delta) = F(1 + \mathrm{Re}[Ve^{(-ik\delta)}]) \tag{2.9}$$

where F simply denotes the total flux obtained from the two apertures.

Here we have introduced the fundamental measurement parameter of an interferometer, V, known as the complex visibility. This is given by

$$V = \int I(\mathbf{\Delta s}) e^{-ik(\mathbf{s_0} \cdot \mathbf{B})} d\Omega \tag{2.10}$$

$$V(u, v) = \int I(\alpha, \beta) e^{-2\pi i(\alpha u + \beta v)} d\alpha d\beta, \tag{2.11}$$

where α, β are angles on the sky and u, v are spatial frequencies defined by:

$$u \equiv \frac{kB_x}{2\pi} \qquad\qquad v \equiv \frac{kB_y}{2\pi}. \tag{2.12}$$

Hence, the complex visibility can be interpreted as a sample from the two dimensional Fourier transform of the source brightness distribution (Haniff, 2007), and is a relationship commonly known as the van Cittert-Zernike theorem (Cittert, 1934; Zernike, 1938). A measurement of the complex visibility can be recovered to within a constant if $i(\mathbf{s_0}, \mathbf{B}, \delta)$ is measured at multiple delays δ. Furthermore if multiple measurements of V can be taken on different baselines, theoretically it is possible to recover an image of the object. Splitting the complex visibility into a modulus $|V|$ and phase ϕ component, we arrive at a detector intensity of:

$$i(\mathbf{s_0}, \mathbf{B}, \delta) \propto 1 + |V| \cos(k\delta + \phi) \tag{2.13}$$

Here, we see that the visibility modulus simply affects the amplitude of the fringes, equivalent to the definition of the visibility by Michelson (1920):

$$|V| = \frac{i_{\text{max}} - i_{\text{min}}}{i_{\text{max}} + i_{\text{min}}} \tag{2.14}$$

Of course, this is assuming monochromatic light and interferometers function with a finite bandpass. Buscher and Longair (2015d) also shows that for a rectangular response function over a bandpass $\Delta\lambda$ centred at a wavelength λ_0 (with equivalent wavenumber k_0), the polychromatic intensity is proportional to:

$$i \propto 1 + \text{sinc}\left(\frac{\delta\Delta\lambda}{\lambda_0^2}\right)|V|\cos\left(k_0\delta + \phi\right) \tag{2.15}$$

Hence, the polychromatic response simply modulates the fringes by a sinc function with a characteristic scale of $\Lambda = \frac{\lambda_0^2}{\Delta\lambda}$, known as the coherence length. In order to have maximum power in the fringes, the delay δ must be set as small as possible, while still being able to be modulated. As δ approaches Λ, the power decreases until falling to zero when the delay equals the coherence length. A schematic of this phenomena is found in Figure 2.2, where the coherence length is the position where the polychromatic fringe goes to zero.

2.2 The Turbulent Atmosphere and Fringe Tracking

Unfortunately, the maths described in the previous section is an ideal case, whereas on the ground one has to deal with the effects of the atmosphere. The atmosphere is turbulent, causing patches of air to vary randomly in temperature and pressure. As the temperature and pressure then affect the refractive index of air, this causes the light passing through to be disturbed, resulting in a corrugated wavefront and a phenomenon known as "seeing". Seeing will cause light observed by a telescope to have a phase offset that varies spatially and temporally. Interferometers are affected differently by atmospheric seeing compared to their monolithic cousins: whereas a single telescope will experience a loss in resolution, an interferometer will see a loss of sensitivity.

The strength of turbulence can be characterised spatially by the Fried parameter r_0, which determines the spatial scale at which the phase variation caused by the atmosphere is 1 radian. Perhaps more pertinent though is the temporal evolution of the turbulence. The frozen turbulence hypothesis states that most temporal variation is caused by the bulk motion of the atmosphere being blown by the wind (Buscher and Longair, 2015a). If there is only one layer of turbulence moving at a speed v, the phase variation can be characterised by the coherence time defined as (Monnier, 2003):

$$t_0 = 0.314 r_0 / v \tag{2.16}$$

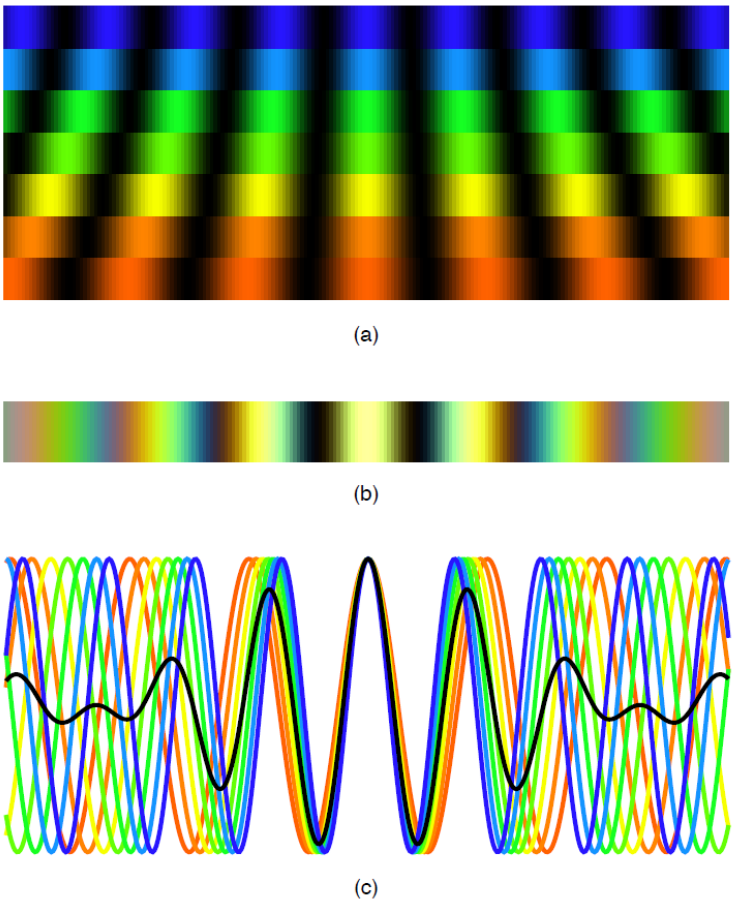

Figure 2.2: Polychromatic fringes. a) Fringes as seen at 7 single wavelengths. b) A polychromatic fringe generated by summing the single wavelength fringes. c) A cross section of the fringes, showing that the polychromatic fringe is modulated by a sinc function due to the differing responses of each component wavelength. Retrieved from Lawson (2000).

For multiple layers, one can use an effective windspeed based on the weighted average of the different layers. This coherence time defines the timescale at which the phase changes by 1 radian, and is usually on the order of a few milliseconds (Buscher and Longair, 2015a). Here we can see the main problem: one must take exposures on a timescale less than the coherence time to avoid the fringes from blurring due to the changing phase of the atmosphere. This means that far fewer photons will be obtained per exposure compared to the typical tens of seconds exposures taken by single aperture telescopes.

The varying nature of the fringe phase due to the atmosphere means it is also impossible to recover the phase of the visibility with two apertures. There are techniques to recover the phase with more apertures (closure phase (Jennison, 1958; Baldwin et al., 1986; Monnier, 2000), differential phase (Petrov et al., 2007; Buscher and Longair, 2015a)) but this is beyond the scope of the project.

Hence the main observable that can be recovered with a two aperture interferometer is the visibility modulus $|V|$, or more precisely the squared visibility modulus $|V|^2$.

Though taking exposures with a duration less than a coherence time will prevent the fringes from smearing, in order to achieve a high signal to noise many exposures will have to be averaged together. This means that the temporal evolution of turbulence will still have to be corrected for to at least some degree. The effect of a phase error in the atmosphere can translate into an optical delay error in the interferometer (that is, light through some part of the atmosphere will travel slightly further than through another part), and so can be corrected with a delay line. This is a translatable stage that can quickly change the optical path inside of the interferometer to compensate for the error induced by the atmosphere. This correction is a form of adaptive optics known as "fringe tracking" and comes in two flavours: phase tracking and group delay tracking. The following is based on Lawson (2000) and Buscher and Longair (2015c).

Phase tracking involves keeping the delay error to within one radian; that is, making sure that the fringes are within one wavelength of their position if the atmosphere was absent (where the visibility is maximum). A type of phase tracking is known as phase unwrapping, where the fringes are modulated (through a change in delay) fast enough such that the atmospheric errors are constant. This requires a modulation time of $\leq t_0/2$, and so is restricted to bright sources. However, with such a scheme, if one has a dedicated fringe tracking detector, the science detector can have longer exposures as the phase error will not influence measurements substantially.

Group delay tracking relies on the fact that the fringes at different wavelengths will have different periods. If one can disperse the light into different wavelength channels (creating a so called "channelled spectrum" (Lawson, 2000)), one can then disentangle the delay where all the wavelength channels have equal intensity - this is the true location of zero delay, and the offset is due to the atmosphere. With this method, the disturbances can be followed without the requirement for keeping the error to within one wavelength, and instead the requirement becomes that one needs to keep the error to within the coherence length Λ. The downside is that group delay tracking does not follow the atmospheric phase, and so the science exposures are still limited to being less than a coherence time. Part of this proposal involves doing a trial study on the numerous algorithms surrounding both phase and group delay tracking.

2.3 Beam Combination

When it comes to combining the light from multiple telescopes, there are a number of ways to achieve this. The first way is to combine the light in free space, using mirrors and lenses to make the beams overlap resulting in interference. There are also two ways to encode the fringes; that is, two

ways of which to detect the sinusoid characteristic of interference. A more thorough treatment of these two methods can be found in Buscher and Longair (2015b) and Minardi et al. (2016).

The first is to directly combine the light on the detector and see the sinusoid on the detector, known as spatial encoding. By measuring the frequency of the fringe and intensity difference between pixels, one can then reconstruct the sinusoid and recover the visibility. Beam combiners using this encoding include *MATISSE* (Lopez et al., 2014) and the now decommissioned *AMBER* (Petrov et al., 2007) on the Very Large Telescope Interferometer (*VLTI*).

However, the amount of light that an interferometer receives is very low, and another way to "encode" the fringe is known as temporal encoding. Here, the light from the two arms of the interferometer are co-axially combined at a beamsplitter, resulting in a beam with uniform intensity. These beams can then be detected with a single pixel detector. To reconstruct the fringe, if one arm of the interferometer is changed with time, then the phase difference of the two arms of the interferometer will change and so the intensity on the detector will vary sinusoidally with time. This has the advantage of having a higher signal to noise due to using one pixel, but has the disadvantage that multiple measurements have to be made within a coherence time due to the modulation of the optical path. The *COAST* (Haniff et al., 2004) and *NPOI* (Armstrong et al., 1998) interferometers used such a scheme to encode the fringes.

As mentioned when discussing the polychromatic response of an interferometer, the fringes will be modulated by a sinc function that is dependent on the size of the bandpass. Furthermore, chromatic dispersion will be inherently present within the optics of the interferometer. Hence, it makes instrumental sense to split the light coming from the star into narrow wavelength channels. From an astrophysics standpoint, this also allows the wavelength dependent nature of the object to be studied. There are multiple ways to do this, such as putting a filter in front of the detector, taking a measurement, and then repeating with a different filter (Buscher and Longair, 2015b). If the beam combiner is temporally encoded with a co-axial configuration, another method is to simply put a prism after the beam is combined and spectrally disperse the fringes on the detector. Such a setup can be seen in Figure 2.3. If one wanted to observe polarisation dependence of an astrophysical source, a Wollaston prism could also be inserted between the point of combination and the detector.

The use of guided optics and optical fibres provide another method of beam combination with numerous advantages. First, if single mode fibres are used for propagation, then the fibres spatially filter out turbulent modes caused by the atmosphere, leaving the fundamental mode to be combined coherently (Coudé du Foresto et al., 1997). In this way, turbulence does not affect the ability to interfere the light, but instead affects the amount of light that can be injected into the fibres. Essentially, the phase fluctuations are turned into intensity fluctuations that are much more easily calibrated. One of the first beam combiners to use optical fibres was *FLUOR* (Coudé du Foresto

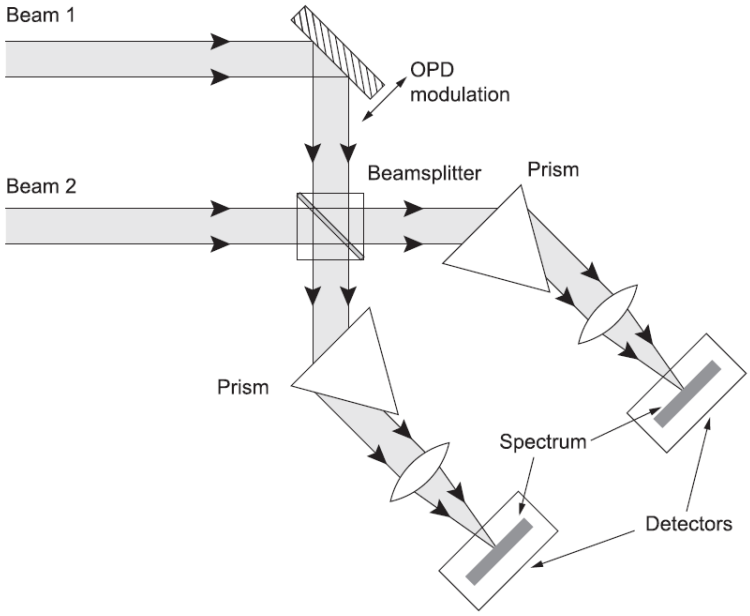

Figure 2.3: A spectrally dispersed temporally encoded beam combiner (Buscher and Longair, 2015b).

et al., 1998), which used a 2x2 optical fibre coupler instead of a beam splitter. However, the fact that there were only two outputs still required the use of temporal delay modulation.

Integrated optics (IO) allow optical waveguides to be etched into a small piece of glass, essentially the equivalent of integrated circuits (Buscher and Longair, 2015b). Complex guides can be built onto a single chip, which has led to great leaps in beam combination. For example, the *GRAVITY* (Abuter et al., 2017) and *PIONEER* (Bouquin et al., 2011) beam combiners for the *VLTI* use a complex IO chip to produce four outputs for each pair of telescopes. As the *VLTI* utilises four telescopes with 6 baselines between them, the chip has 24 outputs in total (seen in the *GRAVITY* IO chip in Figure 2.4). The outputs (denoted A, B, C and D) measure the light with phase offsets of 0, 90, 180 and 270° respectively, which can then reconstruct the complex visibility without the use of temporal fringe scanning as such:

$$V = \frac{A - C + i(B - D)}{A + B + C + D} \tag{2.17}$$

This is quite the advantage as a lack of modulation means that the entire coherence time can be spent on one measurement, resulting in a higher signal to noise. Furthermore, these IO chips can be made to be very small and so work very well under tight volume constraints. The downside to this method is the complexity in the chip, which reduces the throughput of the beam combiner and also can be quite expensive.

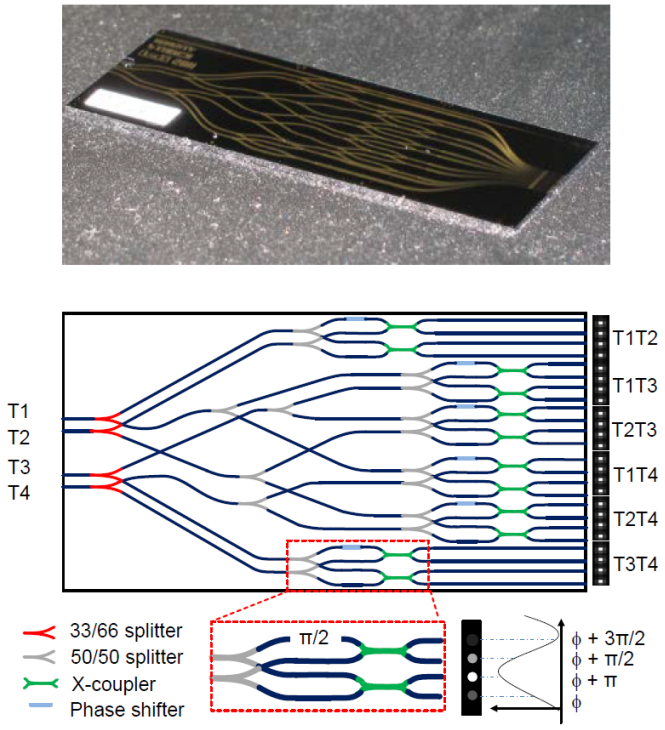

FIGURE 2.4: Photo and schematic of the *GRAVITY* IO beam combination chip (Abuter et al., 2017).

Part of my proposed project will be investigating which beam combination method will be best for the *Pyxis* interferometer, juggling performance with the cost of manufacturing a complex IO chip.

Section 3

The *Pyxis* Interferometer

The next section will delve into the details of what I plan to achieve with this PhD project, in particular the instrumentation component concerning building an interferometric beam combiner from scratch.

As detailed in Section 1, *Pyxis* is a new interferometer that will be built at the Australian National University. The main aim of this interferometer will be to demonstrate a formation flying architecture that could eventually be used on a CubeSat scale or larger space interferometry mission. As this instrument will be ground-based, the formation flying system will be based around three robotic platforms (two "telescopes" and one central combiner) located in the car park of the Advanced Instrumentation and Technology Centre at Mt Stromlo Observatory. These robotic platforms will be able to move around and self adjust so that the optical path difference between the two arms of the interferometer is roughly zero. The excess delay can then be compensated by a delay line within the beam combiner, a small mechanical component which can adjust the distance that the light travels at sub-micron precision.

A schematic of the interferometer can be seen in Figure 3.1 from Ireland (2019). In the schematic, we can see that the interferometer can be broadly broken down into five subsystems:

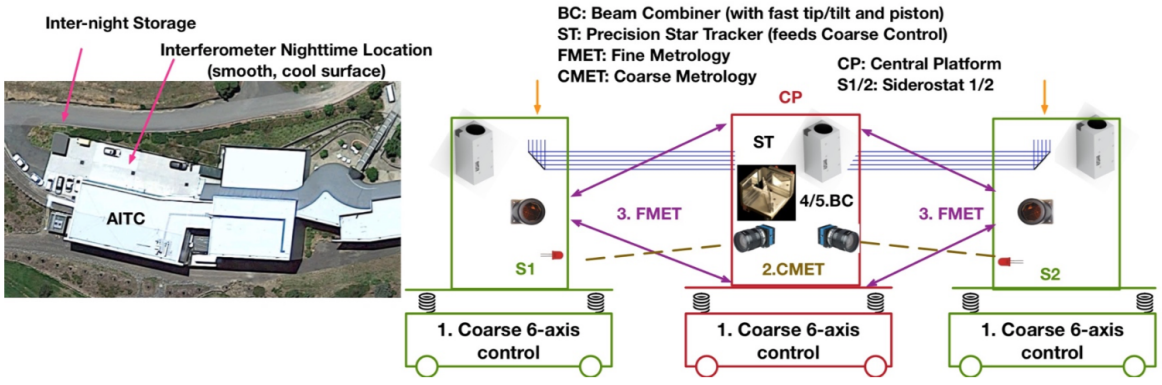

Figure 3.1: Schematic of the *Pyxis* interferometer, along with its potential location. Retrieved from Ireland (2019).

(1) Coarse Mechanical Control: this subsystem consists of the robotic control of the platforms, as well as star tracking (knowing the location of the source the instrument is looking at) and power systems. This subsystem is not directly translatable to space interferometry.
(2) Coarse Metrology: this subsystem aims to identify the relative positions of the two telescopes with regards to the main platform with rough precision. This aims to be achieved by imaging an LED signal originating from the two telescope platforms.
(3) Fine Metrology: perhaps the most novel of the subsystems, this is the most important with regards to space interferometry technology development. This is achieved through combining light reflected off of the two side platforms and analysing the fringes generated (essentially an interferometer within an interferometer). This will provide a far more precise estimate of the relative position of the platforms, which is vital in a formation flying context.
(4) Tip/Tilt Pupil Control: This system aims to correct the low order spatial aberrations caused by the atmosphere so as to inject as much light into the fifth subsystem.
(5) Science Beam Combination: The final subsystem is arguably the most important with regards to *Pyxis* being a stand alone interferometer. This system will take the light collected from the two side platforms and combine it into fringes, so that scientific measurements can be made (as described in the previous section). This component will also be in charge of fringe tracking - performing fine adjustments of the optical path in response to the turbulence in the atmosphere.

The primary goal of my PhD project covers the fifth of these subsystems - designing the scientific beam combiner with the aim to recover scientific information from an astrophysical source. The following subsections will detail the breakup of sub-projects and papers that I aim to complete with regards to the beam combiner. However, I will also play a large roll in integration, testing and debugging of *Pyxis* as a whole and ensuring it is ready to go on sky.

3.1 The Beam Combiner

From the outset, the first (and longest) sub-project will be designing and building the beam combiner itself. This will involve purchasing optical and photonic components and assembling a lab prototype that will take light from two inputs (simulating the two arms of the interferometer) and combining them onto a detector where visibility measurements can be made. Due to volume constraints, it is critical to make the optics as small as possible. This will also help in transferring the technology to a CubeSat scale system.

A block diagram of the function of the beam combiner is shown in Figure 3.2. Like with *Pyxis* as a whole, the beam combiner can be split up into five subsystems, which are explained below:

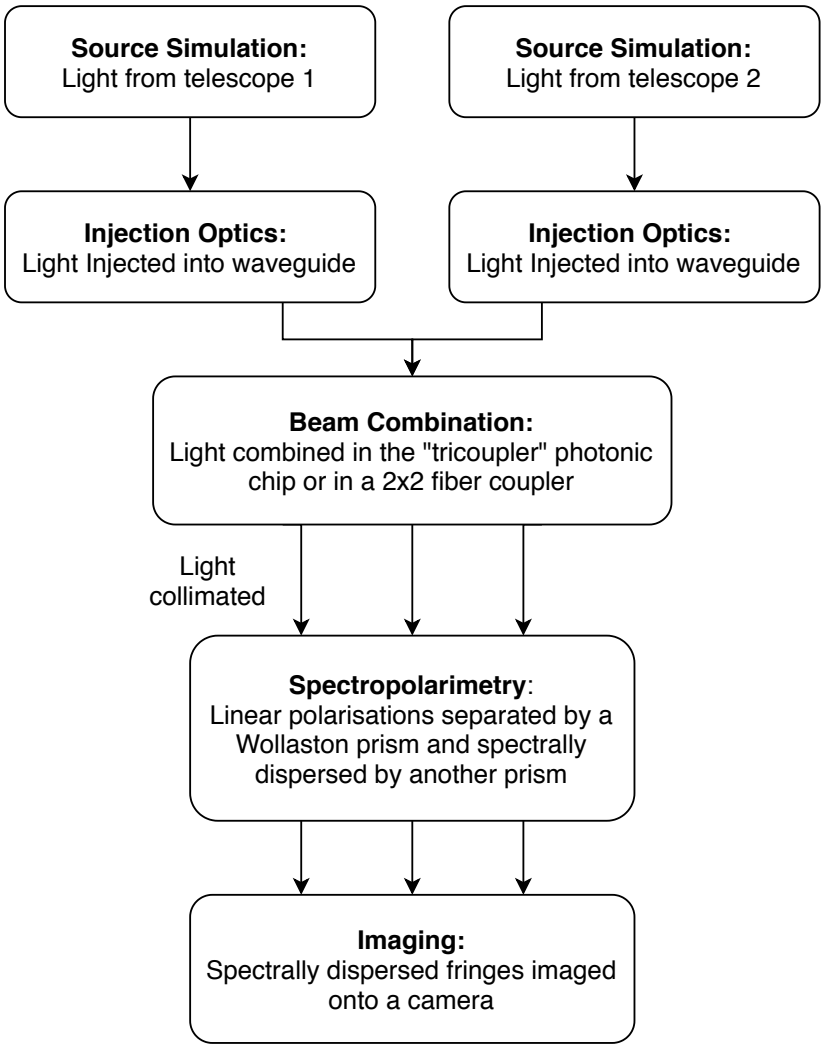

Figure 3.2: Potential block diagram of the *Pyxis* beam combiner.

(1) Source simulation: A small setup consisting of a light source and a beamsplitter that will replicate the light coming from the two arms of the interferometer. This component is for lab testing only, and won't be needed for the final combiner (as the final input will be the starlight reflected off the two telescopes).
(2) Injection optics: An optical setup designed to take the beams coming from the two arms of the interferometer and focus them into waveguides (a photonic system designed to propagate light through a glass path like an optical fibre).
(3) Beam combination: This subsystem mainly consists of photonics designed to combine the light from the two arms. There are two options that I will explore: a tricoupler (discussed in Section 3.1.2) and a simple 2x2 fibre coupler. Both of these options combine the light

from two inputs, and produce two to three outputs that should contain interferometric fringes. These outputs are then collimated before entering the next subsystem.

(4) Spectropolarimetry: This simply consists of a few prisms designed to take the interfered light and disperse it spectrally, as well as separate the two linear polarisations of the light (such as with a Wollaston prism). Our aim is to have a spectral resolution on the order of $\lambda/\Delta\lambda \approx 70$, but we also hope to have a few versions of this module that will allow for other spectral resolutions. Due to the space constraint, it is likely that the best way to mount these prisms will be through 3D printing a small mount that can be attached to the imaging camera in the final subsystem.

(5) Imaging: This simply involves a lens and a camera. However, due to the low number of photons, it is critical that the camera has a very small amount of read-out noise. It is also important that the small part of the detector which will record the fringes is read out very quickly so that one exposure is less than a coherence time (which is on the order of a few milliseconds).

Once a lab prototype can be made and tested, a final version will be constructed before being integrated into the system as a whole (which will likely occur about two years into the PhD). This final version will be missing the first of the subsystems described above, as the injected light will come from the tip/tilt pupil control subsystem. After integration, the whole instrument can be tested on sky before initiating scientific measurements about two and a half years from the start of the project.

My goal will be to write a paper on the design and performance of the beam combiner, which will likely be written at a similar time to the design documents of the other subsystems (at the time of integration). Out of necessity then, this will likely be the final instrumentation paper written for the PhD.

3.2 Investigating the "Tricoupler"

In the process of designing the beam combiner, there are a number of choices to be made. In particular, the actual method of combination is important to consider. As mentioned in Section 2, there are a number of ways to combine the light, including free space optics, guided fibre couplers and photonic chips. Due to *Pyxis* being located at Mt Stromlo (with poor seeing), as well as having small (around 10 cm) apertures, it is important that we collect as many photons as possible. In this manner, there are two options to consider: a simple 2x2 fibre coupler (similar to the FLUOR instrument (Coudé du Foresto et al., 1998)), and a novel coupling method that we have dubbed a "tricoupler".

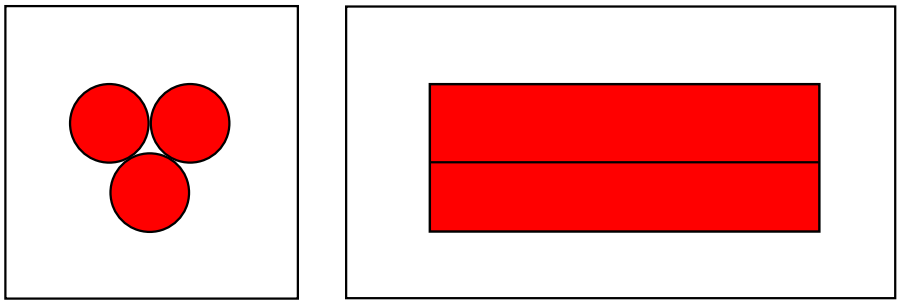

Figure 3.3: A very simple face-on and side-on view of the tricoupler, showing the 3D layout of the waveguides.

The tricoupler is a set of three waveguides (a class of photonic elements such as optical fibres) that are imprinted on a integrated optics (IO) photonic chip, and is designed to take two inputs and provide three outputs. The light in such a device is combined by funnelling the waveguides close to each other, which couples the fields between the different waveguides, before splitting them again. These outputs will be phase shifted from each other by $\frac{2\pi}{3}$, which allows us to recover the complex visibility relatively easily through the relation (where A, B and C are the three outputs):

$$V = \frac{3A + \sqrt{3}i(C - B)}{A + B + C} - 1 \tag{3.1}$$

In order for this to occur, the waveguides must be arranged in three dimensions (as seen in Figure 3.3) rather than in a planar arrangement. While this is relatively difficult to manufacture, our group has contacts with the photonics group at Macquarie University, who have the capability to build such an IO chip. Such a chip has not been used in a interferometer before, although there have been explorations into planar tricouplers for stellar interferometry (e.g. Labeye et al., 2004; Lacour et al., 2014), and such devices are already implemented in quantum optics applications (e.g. Chung et al., 2012).

Hence, a sub-project will be to explore the feasibility of using such an IO chip for *Pyxis*. On the outset there are numerous advantages; in particular, the tricoupler has the ability to recover the full complex visibility instantaneously like the ABCD combiner (e.g Abuter et al., 2017), while having 33% more throughput and being much less complex of an optical device. The throughput is especially important, as we need to recover as much light as possible in our short exposures. However, as it hasn't been developed or made, we are not sure whether the device will work as we hope. Due to the novelty of the tricoupler and the potential advantages is brings, I expect to be able to write a paper on this investigation regardless on whether such a photonic device works in the way we expect or not.

3.3 Designing a Fringe Tracking Algorithm

The final sub-project will involve investigating fringe tracking algorithms. As mentioned in Section 2, there are a variety of methods used to track the optical path disturbances caused by the atmosphere. In particular, there are algorithms for phase tracking (keeping the optical path difference to within one wavelength) and group delay tracking (keeping the delay to within one coherence length). Many beam combiners use different methods, but there is nowhere in the literature that does a complete study on the advantages and disadvantages of each.

In this sub-project, I will aim to develop the maths behind the errors in each of the two types of tracking, to identify which method provides the best way forward in terms of mitigating atmospheric phase error. Furthermore, I hope to compare the reliability of various algorithms for group tracking in particular, as the two different options for *Pyxis'* beam combination will require different algorithms for tracking. While the tricoupler option will allow classical algorithms to be used (such as those proposed in Buscher and Longair (2015c)), the 2x2 coupler requires a delay modulation to retrieve the full complex visibility and hence classical fringe tracking. However, there is an open question as to whether fringe tracking can be accomplished without delay modulation using just two outputs and some purposefully added dispersion. If fringe tracking is possible with this method, then the 2x2 coupler will allow for a 150% increase in photons over the tricoupler.

The visibility modulus (not the full complex visibility) can be estimated with the 2x2 coupler also without modulation, relying on the fact that phase variations between exposures should vary randomly due to the atmosphere. Over a number of exposures, the visibility modulus can be estimated through (assuming outputs of A and C):

$$|V|^2 \approx \frac{\langle (A-C)^2 \rangle}{\langle A+C \rangle^2}$$

where $\langle\rangle$ represent a running average.

A paper exploring these options in fringe tracking algorithms will be a very useful addition to the literature on this topic. Plus, in examining the options for fringe tracking, an informed choice can be made on which waveguide configuration is best.

Section 4

Pyxis Science

My PhD proposal is not solely instrumentation/technology based, as I hope to also take scientific measurements with *Pyxis* and add to the literature on the scattered light structures around giant stars. This section will detail the scientific objectives I hope to explore with *Pyxis*, in particular using interferometric polarimetry, as well as discussing a backup scientific proposal in case of a catastrophic failure of the instrument. It is my goal to produce papers on one to two of the following science targets, depending on the sensitivity that *Pyxis* ends up achieving.

4.1 Background on Optical Interferometric Polarimetry

Optical interferometry has provided great leaps in many areas of astrophysics; particularly in determining the precise diameters of stars (e.g. Rains et al., 2020). However, there is an area of astrophysics for which sufficiently capable interferometers can provide unique astrophysical insight: polarimetric interferometry. This is a technique by which the high resolution of interferometry is paired with the insight gained through measuring the difference in the polarisation states of light (Elias et al., 2008). This can be especially powerful if combined with a spectral analysis through measuring the signal in discrete narrow wavelength channels. This technique is explained in depth in (eg. Ireland et al., 2005; Elias, 2001).

Often, dust surrounding a star (particularly the dust lying close to the photosphere) has a low enough surface brightness that it is indistinguishable from radiation coming from the star (Hough, 2006), and so investigations using photometry and spectroscopy would be difficult at best. In fact, in the optically thin and geometrically extended limit, this scattering dust will not affect photometry and spectroscopy at all as scattering only changes the angle of the outgoing light and not the wavelength of emission. Hence, an important use of polarimetry in astronomy is that of identifying such dust through scattering. In the Rayleigh limit, when light from a star is scattered by material surrounding the source, the light from small particles is orthogonally polarised to the plane containing the scatterer, source and observer (Ireland et al., 2005). An example diagram of this can be seen in Figure 4.1. Furthermore, if the material surrounds the star as a disk, the intensity of the polarisation gives a clue as to the inclination of the disk and due to the wavelength dependence of

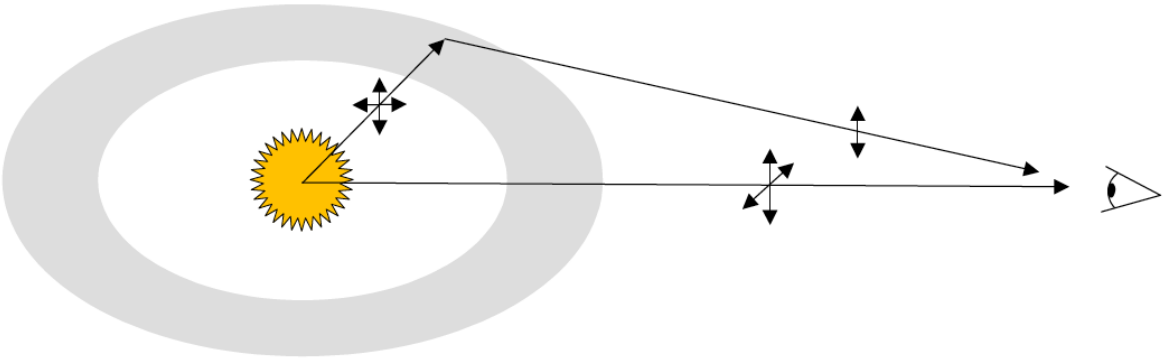

FIGURE 4.1: Example geometry of a circumstellar disk that would give rise to preferential linear polarisation (Keller, 2008)

the scattering, the size of the grains can also be distinguished if viewed in multiple spectral channels (Hough, 2006). Essentially, the light scattered off the dust should be highly polarised compared to the radiation from that star and thus should be visible to a polarimeter.

Of note is the *SPHERE/ZIMPOL* instrument on the Very Large Telescope (*VLT*) (Beuzit et al., 2008). This is a high contrast polarimeter that has produced some very high impact science in imaging planetary systems around other stars (eg. Keppler et al., 2018; Benisty et al., 2015). However, arguably the biggest weakness of this instrument is its resolution - the telescope just doesn't have a large enough diameter to extract many of the signals close to the star. The closest one can get is an angular separation of 27 mas away from the star (e.g Benisty et al., 2015), when the telescope is pushed to its limit.

This highlights a problem that arises for most polarimeters: if the material around a star is axisymmetric, then a polarimeter from a classical telescope will still recover a net zero polarisation as the star is unresolved. This symmetry can be broken by resolving a star with an interferometry, hence leading to a niche that interferometric polarimetry can fill. Taking polarimetry measurements with an interferometer allows the structure of a dusty envelope around a star to be probed in a way that is impossible to probe otherwise. With Pyxis, we can expect at least twice the resolution of *SPHERE*, although we will not achieve anywhere near the sensitivity. In general, the success of high contrast polarimetry coupled with the lack of high angular resolution instruments presents a compelling case for optical interferometric polarimetry.

4.2 Scattered Light Structures around M Giants (and Supergiants)

The first use of interferometric polarimetry was by Ireland et al. (2005), who used the *SUSI* interferometer with some additional polarisers to study the dust around the Mira variables R Car and RR Sco. Mira variables are very red Asymptotic Giant Branch (AGB) stars that undergo long (<100 days) pulsations. The nature of these pulsations is tied to theories of mass loss, where the star sheds material into a circumstellar envelope (see Höfner and Olofsson, 2018; Ireland and Scholz, 2006). However, the nature and mechanism of this process is mired in uncertainties. The study by Ireland et al. (2005) managed to separate the dusty envelope from the photospheric emission, and found that the dust formed at a distance less than three stellar radii. The transparency and spatial structure of this dust was evidence of the complexity of the circumstellar environment around these stars.

Another study by Norris et al. (2012) also used interferometric polarimetry to study Miras, albeit a variant using a technique known as "aperture masking" on the *VLT*. This technique converts what is normally an 8m single aperture into an array of smaller interferometers. In this manner, one can achieve diffraction limited measurements from the ground (although not at the spatial resolution that a long baseline interferometer such as *SUSI* or *Pyxis* could achieve). The results of this study found dust located even closer to the star with surprisingly large sizes, leading to the conclusion that these dust grains must be transparent to the starlight in order to escape sublimation from the radiation.

I hope to continue these investigations into the circumstellar environments of Mira variables using *Pyxis*. These stars are ideal candidates - namely because they are very bright and are very interesting canditates to study using interferometric polarimetry. By hopefully targeting a number of Miras, I hope to further constrain the size and shape of these envelopes, as well as their size distribution and composition (achievable due to the spectral component of *Pyxis*). In this manner, I will be able to provide some new insight into the mechanisms concerning how AGB stars undergo mass loss and the nature of the dust surrounding them.

Another similar avenue of science that I could take data on is investigating the relationship between temperature and dust formation. A question regarding the highest temperature at which dust can form around M giants/supergiants could be looked at through taking high resolution polarimetric measurements around many M giants and supergiants such as Betelgeuse and Antares. This would also be able to provide insight into whether the temperature of a star plays a role in affecting the ability of a star to drive wind through its scattering (Höfner and Olofsson, 2018). Betelgeuse is also an interesting target due to the great dimming that occurred at the end of 2019 before reaching a minimum in late February. This was heavily reported in popular media and many researchers have attributed this to a dust envelope in our line of sight (see Levesque and Massey, 2020; Safonov et al.,

2020). Attempting to resolve this in scattered light (such as done by Kervella et al. (2016), albeit with a higher resolution) could determine how far above the photosphere any dust present forms.

4.3 Stretch Goal: Herbig Ae/Be Stars

The biggest challenge scientifically for *Pyxis* will be aiming for a relatively high sensitivity and hence a larger magnitude limit. This greatly restricts the possible science that can be done, as the number of interesting science cases that can be pursued with a reconfigurable interferometer with a polarimeter increases exponentially with the magnitude limit.

One potential stretch goal, if we can push *Pyxis* to extract visibilities with a decent signal to noise ratio for stars of magnitudes around magnitude 6, is to look at Herbig Ae/Be stars. These are very young giant stars that still contain a protoplanetary disk, and so are great targets for studying the process of star and planet formation. One star in particular would be worth looking at: 51 Ophiuchi. This is a very bright Herbig Be star in the southern hemisphere, and is known to have a compact disk that can only be resolved by interferometry (Stark et al., 2009). Analysing the spatial structure and composition of the disk with polarimetric measurements will help provide more insight into planet formation, in particular with regards to the role of transparent dust in the inner recesses of a young star's disk. Furthermore, if an inclination can be determined through polarimetry to an acceptable precision, it can be paired with the work from Jenkins and Gry (2020) to constrain the scale height of molecular material in the disk.

4.4 Backup Science with the *VLTI*

Of course, things may not go to plan and the *Pyxis* instrument may encounter major difficulties. Over the next six months, hopefully key risks in the metrology and vibration control systems are resolved, but this is not guaranteed due to the experimental nature of the project. In the case that I am unable to undertake scientific measurements with *Pyxis*, I have a contingency plan through a proposal for the Very Large Telescope Interferometer (*VLTI*) submitted in this current semester. This proposal consists of observations of the Mira variable T Lep with the *MATISSE* instrument, aiming to resolve dust and molecular shells in the near to mid infrared. Such a proposal is very complementary to the science proposed in *Pyxis*, as we can investigate both the thermal emission from dust through the *VLTI* proposal, as well as the transparent dust with a polarimeter such as *Pyxis*. If *Pyxis* does not manage to reach the science stage by the end of my candidature though, this proposal should be sufficient to provide me with some data analysis and a paper on a topic similar to what I would have planned to investigate otherwise.

Section 5

Research Plan

5.1 Supervisors

A list of my proposed supervisors is found in Table 5.1.

Table 5.1: Supervisory Panel

Position	**Name**	**Expertise**
Primary Supervisor	A/Prof Michael Ireland	Interferometry, Photonics, Mira variables
Associate Supervisor	Dr Tony Travouillon	Photonics, Systems Engineering
Associate Supervisor	Dr Tiphaine Lagadec	Photonics, Day to day lab work

5.2 Potential Risks

A list of potential PhD risks and methods to mitigate them are found in Table 5.2.

Table 5.2: Risk Register

Description of risk	**Mitigation**
Procurement delay of parts and equipment	Aim to purchase parts early
Requiring specialists/equipment that are unavailable for a period of time	Try alternative avenues; have other subprojects to work on in the meantime
Delays caused by resurgence in the COVID-19 disease and related travel restrictions	Cannot mitigate - potential extension of PhD
Waiting on other subsystems that are delayed before integration, halting progress	Have other subprojects to work on in the meantime
Technology Failure: Parts of the instrument simply don't work as we require	Resort to backup projects (eg. *VLTI* proposal)
Vibrations of Pyxis too high/ Magnitude limit too low for science/ Failure of Pyxis telescope design	Write demonstration papers, resort to *VLTI* proposal project

5.3 Timeline

A proposed timeline for the PhD is shown in Table 5.3.

Table 5.3: Research Timeline

Date	Description
2020	
February	Start PhD
July	Submit and present proposal
August	Basic lab setup completed
November	Attend and present at Mt Stromlo Student Seminars
December	*LIFE* workshop (COVID pending)
	Attend and present at SPIE 2020 (COVID pending)
2021	
January	Attend and present at COSPAR 2021 (COVID pending)
February	**1 Year**
	Draft of tricoupler paper
May	Final beam combiner design
June	Attend and present at ASA 2021
	Draft of fringe tracking paper
July	Annual review
	Assess whether the backup *VLTI* observations will be necessary
September	Assemble final beam combiner to begin integration
November	Attend and present at Mt Stromlo Student Seminars
December	Attend and present at AIP National Congress 2021
2022	
February	**2 Years**
March	End integration and testing
April	Draft of beam combiner paper
	Begin science measurements
May	Begin writing up thesis
June	Attend and present at SPIE 2022
	Attend and present at ASA 2022
July	Annual review
November	Draft of science paper
	Attend and present at Mt Stromlo Student Seminars
2023	
February	**3 Years**
	Final submission
	Final thesis seminar
July	**3.5 Years**
	Buffer time available for if things go wrong

Bibliography

Abuter, R. et al. (June 2017). 'First light for GRAVITY: Phase referencing optical interferometry for the Very Large Telescope Interferometer'. en. In: *Astronomy & Astrophysics* 602. Publisher: EDP Sciences, A94. ISSN: 0004-6361, 1432-0746. DOI: 10.1051/0004-6361/201730838. URL: https://www.aanda.org/articles/aa/abs/2017/06/aa30838-17/aa30838-17.html (visited on 29/05/2020).

Angel, J. R. P. and N. J. Woolf (Jan. 1997). 'An Imaging Nulling Interferometer to Study Extrasolar Planets'. In: *The Astrophysical Journal* 475.1, pp. 373–379. ISSN: 0004-637X. DOI: 10.1086/303529. URL: http://stacks.iop.org/0004-637X/475/i=1/a=373.

Armstrong, J. T. et al. (Mar. 1998). 'The Navy Prototype Optical Interferometer'. en. In: *The Astrophysical Journal* 496.1. Publisher: IOP Publishing, p. 550. ISSN: 0004-637X. DOI: 10.1086/305365. URL: https://iopscience.iop.org/article/10.1086/305365/meta (visited on 29/05/2020).

Baldwin, J. E. et al. (Apr. 1986). 'Closure phase in high-resolution optical imaging'. In: *Nature* 320.6063, pp. 595–597. DOI: 10.1038/320595a0.

Beichman, C. A., N. J. Woolf and C. A. Lindensmith (1999). *The Terrestrial Planet Finder (TPF) : a NASA Origins Program to search for habitable planets*. Tech. rep. Pasadena, California: Jet Propulsion Laboratory, California Institute of Technology. URL: http://adsabs.harvard.edu/abs/1999tpf..book.....B.

Benisty, M. et al. (June 2015). 'Asymmetric features in the protoplanetary disk MWC 758'. In: *Astronomy and Astrophysics* 578, p. L6. ISSN: 0004-6361. DOI: 10.1051/0004-6361/201526011. URL: http://adsabs.harvard.edu/abs/2015A%26A...578L...6B (visited on 24/06/2020).

Beuzit, Jean-Luc et al. (July 2008). 'SPHERE: a 'Planet Finder' instrument for the VLT'. In: 7014. Conference Name: Ground-based and Airborne Instrumentation for Astronomy II, p. 701418. DOI: 10.1117/12.790120. URL: http://adsabs.harvard.edu/abs/2008SPIE.7014E..18B (visited on 24/06/2020).

Boden, A. F. (Jan. 2000). 'Elementary Theory of Interferometry'. In: *Principles of Long Baseline Stellar Interferometry*. Ed. by Peter R. Lawson, p. 9.

Borucki, W. J. et al. (Feb. 2010). 'Kepler Planet-Detection Mission: Introduction and First Results'. In: *Science* 327, p. 977. DOI: 10.1126/science.1185402.

Bouquin, J.-B. Le et al. (Nov. 2011). 'PIONIER: a 4-telescope visitor instrument at VLTI'. en. In: *Astronomy & Astrophysics* 535. Publisher: EDP Sciences, A67. ISSN: 0004-6361, 1432-0746. DOI: 10.1051/0004-6361/201117586. URL: https://www.aanda.org/articles/aa/abs/2011/11/aa17586-11/aa17586-11.html (visited on 29/05/2020).

Buscher, David F. and Malcolm Longair (2015a). 'Atmospheric seeing and its amelioration'. In: *Practical Optical Interferometry: Imaging at Visible and Infrared Wavelengths*. Cambridge Observing Handbooks for Research Astronomers. Cambridge University Press, pp. 53–90. DOI: 10.1017/CBO9781107323933.005.

— (2015b). 'Interferometers in practice'. In: *Practical Optical Interferometry: Imaging at Visible and Infrared Wavelengths*. Cambridge Observing Handbooks for Research Astronomers. Cambridge University Press, pp. 91–128. DOI: 10.1017/CBO9781107323933.006.

— (2015c). 'Interferometric observation of faint objects'. In: *Practical Optical Interferometry: Imaging at Visible and Infrared Wavelengths*. Cambridge Observing Handbooks for Research Astronomers. Cambridge University Press, pp. 152–179. DOI: 10.1017/CBO9781107323933.008.

— (2015d). 'Making fringes'. In: *Practical Optical Interferometry: Imaging at Visible and Infrared Wavelengths*. Cambridge Observing Handbooks for Research Astronomers. Cambridge University Press, pp. 1–35. DOI: 10.1017/CBO9781107323933.003.

Chung, Kelvin et al. (Oct. 2012). 'Broadband and robust optical waveguide devices using coherent tunnelling adiabatic passage'. EN. In: *Optics Express* 20.21. Publisher: Optical Society of America, pp. 23108–23116. ISSN: 1094-4087. DOI: 10.1364/OE.20.023108. URL: http://www.osapublishing.org/oe/abstract.cfm?uri=oe-20-21-23108 (visited on 18/05/2020).

Cittert, P.H van (Jan. 1934). 'Die Wahrscheinliche Schwingungsverteilung in Einer von Einer Lichtquelle Direkt Oder Mittels Einer Linse Beleuchteten Ebene'. In: *Physica* 1.1-6, pp. 201–210. ISSN: 0031-8914. DOI: 10.1016/S0031-8914(34)90026-4. URL: https://www.sciencedirect.com/science/article/pii/S0031891434900264?via%3Dihub.

Cockell, Charles S. et al. (Mar. 2009). 'Darwin—an experimental astronomy mission to search for extrasolar planets'. In: *Experimental Astronomy* 23.1, pp. 435–461. ISSN: 0922-6435. DOI: 10.1007/s10686-008-9121-x. URL: http://link.springer.com/10.1007/s10686-008-9121-x.

Coudé du Foresto, V., S. Ridgeway and J.-M. Mariotti (Feb. 1997). 'Deriving object visibilities from interferograms obtained with a fiber stellar interferometer'. en. In: *Astronomy and Astrophysics Supplement Series* 121.2, pp. 379–392. ISSN: 0365-0138, 1286-4846. DOI: 10.1051/aas:1997290. URL: https://aas.aanda.org/articles/aas/abs/1997/02/ds1170/ds1170.html (visited on 03/02/2020).

Coudé du Foresto, Vincent et al. (July 1998). 'FLUOR fibered instrument at the IOTA interferometer'. In: *Astronomical Interferometry*. Vol. 3350. International Society for Optics and Photonics, pp. 856–863. DOI: 10.1117/12.317153. URL: https://www-spiedigitallibrary-org.virtual.anu.edu.au/conference-proceedings-of-spie/3350/0000/FLUOR-fibered-instrument-at-the-IOTA-interferometer/10.1117/12.317153.short (visited on 03/02/2020).

Diamond-Lowe, Hannah et al. (Sept. 2019). 'Simultaneous Optical Transmission Spectroscopy of a Terrestrial, Habitable-Zone Exoplanet with Two Ground-Based Multi-Object Spectrographs'. In: *arXiv e-prints*, arXiv:1909.09104, arXiv:1909.09104. arXiv: 1909.09104 [astro-ph.EP].

Elias II, Nicholas M. (Mar. 2001). 'Optical Interferometric Polarimetry. I. Foundation'. In: *The Astrophysical Journal* 549, pp. 647–668. ISSN: 0004-637X. DOI: 10.1086/319046. URL: http://adsabs.harvard.edu/abs/2001ApJ...549..647E (visited on 24/06/2020).

Elias II, Nicholas M. et al. (Nov. 2008). 'The case for optical interferometric polarimetry'. In: *arXiv e-prints* 0811, arXiv:0811.3139. URL: http://adsabs.harvard.edu/abs/2008arXiv0811.3139E (visited on 31/05/2020).

Haniff, Chris (Oct. 2007). 'An introduction to the theory of interferometry'. In: *New Astronomy Reviews* 51.8-9, pp. 565–575. DOI: 10.1016/j.newar.2007.06.002. URL: https://linkinghub.elsevier.com/retrieve/pii/S1387647307000619.

Haniff, Christopher A. et al. (Oct. 2004). 'COAST: recent technology and developments'. In: *New Frontiers in Stellar Interferometry*. Vol. 5491. International Society for Optics and Photonics, pp. 511–519. DOI: 10.1117/12.552278. URL: http://www.spiedigitallibrary.org/conference-proceedings-of-spie/5491/0000/COAST-recent-technology-and-developments/10.1117/12.552278.short (visited on 29/05/2020).

Hansen, Jonah (2019). 'A Feasibility Study for an Astrophysical Linear Formation Flying Space Interferometer'. Australian National University.

Hansen, Jonah T. and Michael J. Ireland (2020). 'A linear formation-flying astronomical interferometer in low Earth orbit'. In: *Publications of the Astronomical Society of Australia* 37, e019. DOI: 10.1017/pasa.2020.13.

Höfner, Susanne and Hans Olofsson (Jan. 2018). 'Mass loss of stars on the asymptotic giant branch'. en. In: *The Astronomy and Astrophysics Review* 26.1, p. 1. ISSN: 1432-0754. DOI: 10.1007/s00159-017-0106-5. URL: https://doi.org/10.1007/s00159-017-0106-5 (visited on 09/06/2020).

Hough, James (June 2006). 'Polarimetry: a powerful diagnostic tool in astronomy'. en. In: *Astronomy & Geophysics* 47.3. Publisher: Oxford Academic, pp. 3.31–3.35. ISSN: 1366-8781. DOI: 10.1111/j.1468-4004.2006.47331.x. URL: https://academic.oup.com/astrogeo/article/47/3/3.31/209077 (visited on 31/05/2020).

Ireland, M. J. and M. Scholz (Apr. 2006). 'Observable effects of dust formation in dynamic atmospheres of M-type Mira variables'. In: *Monthly Notices of the Royal Astronomical Society*

367, pp. 1585–1593. ISSN: 0035-8711. DOI: 10.1111/j.1365-2966.2006.10064.x. URL: http://adsabs.harvard.edu/abs/2006MNRAS.367.1585I (visited on 30/06/2020).

Ireland, M. J. et al. (July 2005). 'Dust scattering in the Miras R Car and RR Sco resolved by optical interferometric polarimetry'. en. In: *Monthly Notices of the Royal Astronomical Society* 361.1, pp. 337–344. ISSN: 0035-8711. DOI: 10.1111/j.1365-2966.2005.09181.x. URL: https://academic.oup.com/mnras/article/361/1/337/1023507 (visited on 03/02/2020).

Ireland, Michael (2019). *Pyxis: Robotic Linear Formation Interferometry for Astrophysics*. ARC Discovery Grant Proposal.

Jenkins, Edward B. and Cecile Gry (Apr. 2020). 'The Composition, Excitation, and Physical State of Atomic Gas in the Debris Disk Surrounding 51 Oph'. In: *arXiv e-prints* 2004, arXiv:2004.10238. URL: http://adsabs.harvard.edu/abs/2020arXiv200410238J (visited on 09/06/2020).

Jennison, R. C. (Jan. 1958). 'A phase sensitive interferometer technique for the measurement of the Fourier transforms of spatial brightness distributions of small angular extent'. In: *MNRAS* 118, p. 276. DOI: 10.1093/mnras/118.3.276.

Keller, Christoph (2008). *Exoplanetary Systems in Polarized Light*. URL: https://home.strw.leidenuniv.nl/~keller/exoplanets.shtml.

Keppler, M. et al. (Sept. 2018). 'Discovery of a planetary-mass companion within the gap of the transition disk around PDS 70'. In: *Astronomy and Astrophysics* 617, A44. ISSN: 0004-6361. DOI: 10.1051/0004-6361/201832957. URL: http://adsabs.harvard.edu/abs/2018A%26A...617A..44K (visited on 24/06/2020).

Kervella, P. et al. (Jan. 2016). 'The close circumstellar environment of Betelgeuse. III. SPHERE/ZIMPOL imaging polarimetry in the visible'. In: *Astronomy and Astrophysics* 585, A28. ISSN: 0004-6361. DOI: 10.1051/0004-6361/201527134. URL: http://adsabs.harvard.edu/abs/2016A%26A...585A..28K (visited on 30/06/2020).

Labeye, Pierre R. et al. (Oct. 2004). 'Integrated optics components in silica on silicon technology for stellar interferometry'. In: *New Frontiers in Stellar Interferometry*. Vol. 5491. International Society for Optics and Photonics, pp. 667–676. DOI: 10.1117/12.551863. URL: https://www-spiedigitallibrary-org.virtual.anu.edu.au/conference-proceedings-of-spie/5491/0000/Integrated-optics-components-in-silica-on-silicon-technology-for-stellar/10.1117/12.551863.short (visited on 19/03/2020).

Lacour, S. et al. (Apr. 2014). 'A new interferometer architecture combining nulling with phase closure measurements'. en. In: *Monthly Notices of the Royal Astronomical Society* 439.4, pp. 4018–4029. ISSN: 0035-8711. DOI: 10.1093/mnras/stu258. URL: https://academic.oup.com/mnras/article/439/4/4018/1174583 (visited on 06/04/2020).

Lawson, P. R. (Jan. 2000). 'Phase and Group Delay Estimation'. In: *Principles of Long Baseline Stellar Interferometry*. Ed. by Peter R. Lawson, p. 113.

Léger, A. et al. (Oct. 1996). 'Could We Search for Primitive Life on Extrasolar Planets in the Near Future?' In: *Icarus* 123.2, pp. 249–255. ISSN: 0019-1035. DOI: 10.1006/ICAR.1996.0155. URL: https://www.sciencedirect.com/science/article/pii/S0019103596901554?via%3Dihub.

Levesque, Emily M. and Philip Massey (Mar. 2020). 'Betelgeuse Just Is Not That Cool: Effective Temperature Alone Cannot Explain the Recent Dimming of Betelgeuse'. In: *The Astrophysical Journal Letters* 891, p. L37. ISSN: 0004-637X. DOI: 10.3847/2041-8213/ab7935. URL: http://adsabs.harvard.edu/abs/2020ApJ...891L..37L (visited on 09/06/2020).

Lopez, B. et al. (Sept. 2014). 'An Overview of the MATISSE Instrument — Science, Concept and Current Status'. In: *The Messenger* 157, pp. 5–12. ISSN: 0722-6691. URL: http://adsabs.harvard.edu/abs/2014Msngr.157....5L (visited on 29/05/2020).

Mayor, M. et al. (Dec. 2003). 'Setting New Standards with HARPS'. In: *The Messenger* 114, pp. 20–24.

Mayor, Michel and Didier Queloz (Nov. 1995). 'A Jupiter-mass companion to a solar-type star'. In: *Nature* 378.6555, pp. 355–359. ISSN: 0028-0836. DOI: 10.1038/378355a0. URL: http://www.nature.com/articles/378355a0.

Michelson, A. A. (Jan. 1920). 'No. 184. On the application of interference methods to astronomical measurements.' In: *Contributions from the Mount Wilson Observatory / Carnegie Institution of Washington* 184, pp. 1–6.

Michelson, A. A. and F. G. Pease (May 1921). 'Measurement of the diameter of alpha Orionis with the interferometer.' In: *The Astrophysical Journal* 53, p. 249. ISSN: 0004-637X. DOI: 10.1086/142603. URL: http://adsabs.harvard.edu/doi/10.1086/142603.

Minardi, Stefano et al. (Aug. 2016). 'Beam combination schemes and technologies for the Planet Formation Imager'. In: *Optical and Infrared Interferometry and Imaging V*. Vol. 9907. International Society for Optics and Photonics, 99071N. DOI: 10.1117/12.2232656. URL: http://www.spiedigitallibrary.org/conference-proceedings-of-spie/9907/99071N/Beam-combination-schemes-and-technologies-for-the-Planet-Formation-Imager/10.1117/12.2232656.short (visited on 29/05/2020).

Monnier, J. D. (Jan. 2000). 'An Introduction to Closure Phases'. In: *Principles of Long Baseline Stellar Interferometry*. Ed. by Peter R. Lawson, p. 203.

Monnier, John D (May 2003). 'Optical interferometry in astronomy'. In: *Reports on Progress in Physics* 66.5, pp. 789–857. ISSN: 0034-4885. DOI: 10.1088/0034-4885/66/5/203. URL: http://stacks.iop.org/0034-4885/66/i=5/a=203?key=crossref.c1b6e5c01042f7bcbfcac736c3de1a50.

Monnier, John D. et al. (Dec. 2018). 'The planet formation imager'. In: *Experimental Astronomy* 46.3, pp. 517–529. ISSN: 1572-9508. DOI: 10.1007/s10686-018-9594-1. URL: https://doi.org/10.1007/s10686-018-9594-1.

National Aeronautics and Space Administration (2019). *LUVIOR final report*. Tech. rep. NASA. URL: https://ui.adsabs.harvard.edu/search/q=Luvoir%20final%20report&sort=date%20desc%2C%20bibcode%20desc&p_=0.

Norris, Barnaby R. M. et al. (Apr. 2012). 'A close halo of large transparent grains around extreme red giant stars'. en. In: *Nature* 484.7393, pp. 220–222. ISSN: 1476-4687. DOI: 10.1038/nature10935. URL: https://www.nature.com/articles/nature10935 (visited on 03/02/2020).

Petrov, R. G. et al. (Mar. 2007). 'AMBER, the near-infrared spectro-interferometric three-telescope VLTI instrument'. en. In: *Astronomy & Astrophysics* 464.1. Number: 1 Publisher: EDP Sciences, pp. 1–12. ISSN: 0004-6361, 1432-0746. DOI: 10.1051/0004-6361:20066496. URL: https://www.aanda.org/articles/aa/abs/2007/10/aa6496-06/aa6496-06.html (visited on 29/05/2020).

Quanz, Sascha P. et al. (July 2018). 'Exoplanet science with a space-based mid-infrared nulling interferometer'. In: *Optical and Infrared Interferometry and Imaging VI*. Ed. by Antoine Mérand, Michelle J. Creech-Eakman and Peter G. Tuthill. Vol. 10701. SPIE, p. 37. ISBN: 9781510619555. DOI: 10.1117/12.2312051. URL: https://www.spiedigitallibrary.org/conference-proceedings-of-spie/10701/2312051/Exoplanet-science-with-a-space-based-mid-infrared-nulling-interferometer/10.1117/12.2312051.full.

Quanz, Sascha P. et al. (Aug. 2019). 'Atmospheric characterization of terrestrial exoplanets in the mid-infrared: biosignatures, habitability & diversity'. URL: http://arxiv.org/abs/1908.01316.

Rains, Adam D. et al. (Apr. 2020). 'Precision angular diameters for 16 southern stars with VLTI/PIONIER'. In: *Monthly Notices of the Royal Astronomical Society* 493, pp. 2377–2394. ISSN: 0035-8711. DOI: 10.1093/mnras/staa282. URL: http://adsabs.harvard.edu/abs/2020MNRAS.493.2377R (visited on 31/05/2020).

Safonov, Boris et al. (May 2020). 'Differential Speckle Polarimetry of Betelgeuse in 2019-2020: the rise is different from the fall'. In: *arXiv e-prints* 2005, arXiv:2005.05215. URL: http://adsabs.harvard.edu/abs/2020arXiv200505215S (visited on 09/06/2020).

Shao, Michael (July 1998). 'SIM: the space interferometry mission'. In: *Proc. SPIE*. Ed. by Robert D. Reasenberg. Vol. 3350. Society of Photo-Optical Instrumentation Engineers (SPIE) Conference Series, pp. 536–540. DOI: 10.1117/12.317092.

Stark, Christopher C. et al. (Oct. 2009). '51 Ophiuchus: A Possible Beta Pictoris Analog Measured with the Keck Interferometer Nuller'. In: *The Astrophysical Journal* 703, pp. 1188–1197. ISSN: 0004-637X. DOI: 10.1088/0004-637X/703/2/1188. URL: http://adsabs.harvard.edu/abs/2009ApJ...703.1188S (visited on 09/06/2020).

Zernike, F. (Aug. 1938). 'The concept of degree of coherence and its application to optical problems'. In: *Physica* 5.8, pp. 785–795. ISSN: 0031-8914. DOI: 10.1016/S0031-8914(38)

80203 - 2. URL: https://www.sciencedirect.com/science/article/pii/S0031891438802032?via%3Dihub.